ACS APPLIED MATERIALS & INTERFACES
Research Article
www.acsami.org

Monolithic Composites of Silica Aerogels by Reactive Supercritical Deposition of Hydroxy-Terminated Poly(Dimethylsiloxane)

D. Sanli[†] and C. Erkey*[,†,‡]

[†]Department of Chemical and Biological Engineering, Koç University, 34450 Sariyer, Istanbul, Turkey
[‡]Koç University Tüpraş Energy Center (KUTEM), Koç University, 34450 Sariyer, Istanbul, Turkey

ABSTRACT: Monolithic composites of silica aerogels with hydroxyl-terminated poly(dimethylsiloxane) (PDMS(OH)) were developed with a novel reactive supercritical deposition technique. The method involves dissolution of PDMS(OH) in supercritical CO_2 ($scCO_2$) and then exposure of the aerogel samples to this single phase mixture of PDMS(OH)-CO_2. The demixing pressures of the PDMS(OH)-CO_2 binary mixtures determined in this study indicated that PDMS(OH) forms miscible mixtures with CO_2 at a wide composition range at easily accessible pressures. Upon supercritical deposition, the polymer molecules were discovered to react with the hydroxyl groups on the silica aerogel surface and form a conformal coating on the surface. The chemical attachment of the polymer molecules on the aerogel surface were verified by prolonged extraction with pure $scCO_2$, simultaneous deposition with superhydrophobic and hydrophilic silica aerogel samples and ATR-FTIR analysis. All of the deposited silica aerogel samples were obtained as monoliths and retained their transparency up to around 30 wt % of mass uptake. PDMS(OH) molecules were found to penetrate all the way to the center of the monoliths and were distributed homogenously throughout the cylindrical aerogel samples. Polymer loadings as high as 75.4 wt % of the aerogel mass could be attained. It was shown that the polymer uptake increases with increasing exposure time, as well as the initial polymer concentration in the vessel.

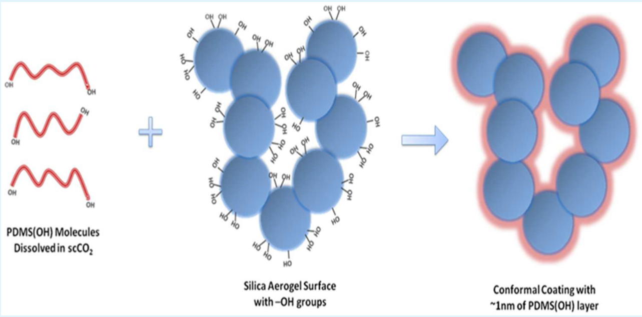

KEYWORDS: *silica aerogel, PDMS(OH), demixing pressure, supercritical deposition, surface modification*

INTRODUCTION

Silica aerogels are nanostructured materials that have been attracting considerable attention because of their unique and intriguing properties, such as low density, transparency, high surface area, high porosity, and low thermal conductivity. More importantly, their properties can be tailored for a specific application either by manipulation of the synthesis parameters during the sol−gel process or by post-treatment of the synthesized aerogels.[1−4] Another important feature of silica aerogels is that they can be obtained as monoliths in any size and shape. Because of these favorable properties, silica aerogels have been utilized or under investigation for various applications, such as thermal insulation, adsorption, nuclear waste storage, electrochemical energy storage, and catalysis.[5]

A significant fraction of the recent studies on silica aerogels are associated with the development of composites of silica aerogels with various polymers. There are different ways to incorporate a polymer into the aerogel structure. One way is to add the polymer to the sol mixture before the gelation occurs, i.e. during the hydrolysis or condensation steps of the sol−gel process. Composites of silica aerogels with poly(2-vinylpyridine),[6] syndiotactic polystyrene,[7] and polyethylene glycol[8] constitute some examples to this technique where gelation occurs in the presence of the polymers chains. By this way, the polymer chains are spread between the silica particles which makeup the network resulting in a composite material with a silica phase and a polymer phase.

An alternative route involves the reaction of the polymer molecules with the surface groups of the silica aerogel which is carried out after the formation of the solid gel network. The hydroxyl groups of the native silica aerogel surface can in principle participate in such reactions. A more commonly used method is to functionalize the aerogel surface with specific chemical groups. The surface functionalization procedure can be performed during the synthesis by adding the appropriate agents into the reactant mixture, or can be carried out as a postgelation treatment by utilizing surface −OH groups of the already formed silica network. Once attached, the functional surface groups constitute active sites for further reactions and are used for the attachment of the polymers. Thus far, there have been many studies on the modification of the silica aerogel surface with various silane based compounds having different functionalities. For instance, amine groups have been introduced to the silica aerogel surface by co-condensation of tetraethylorthosilicate (TEOS) or tetramethylorthosilicate with bis(trimethoxysilylpropyl)amine[9] and 3-aminopropyltriethoxy-

Received: August 13, 2013
Accepted: October 29, 2013
Published: October 29, 2013

silane.[10−12] These amine groups have further been employed for the reactions with isocyanates to yield a coating of polyurea on the aerogel surface. As an alternative method for the coating of the silica network with polyurea, the surface −OH groups were directly employed after the gelation step for the binding of di- or tri-isocyanates.[13,14] Additionally, amine functionalized silica gel surfaces were reacted with different epoxy compounds to yield epoxy reinforced materials.[10,11,15] In all these cases, the polymers were found to coat the surface of the silica particles which make up the silica aerogel network. Such conformal coatings were also achieved with polycyanoacrylates,[16−18] polystyrene,[12,19−21] polymethylmethacrylate,[22] and polyvinyl alcohol[23] by utilizing native or functionalized gel surfaces.

As a third alternative, polymers can be added to the reactant mixture during the synthesis and can directly participate in the co-condensation reactions with the hydrolyzed precursor molecules. This method requires specific polymers that can undergo co-condensation reactions with −OH groups of the hydrolyzed silane precursors. Poly(dimethylsiloxane) (PDMS) with hydroxyl end groups (PDMS(OH)) is one of the rare polymers that can participate in such reactions. Kramer et.al. synthesized a composite of PDMS(OH) with silica aerogel for the first time by reacting the polymer with the hydrolyzed TEOS molecules.[24] After the supercritical extraction of ethanol from the pores, an aerogel composite also termed as “aeromosil” was obtained. The aeromosil had a polymer content up to 20 wt % with improved mechanical properties, however had an opaque appearance. Because it is a water-insoluble polymer, PDMS is quite incompatible with the conventional reactant mixture (ethanol, water, and TEOS) for synthesis of silica aerogels and the addition of the polymer into this mixture causes immiscibility. The immiscibility between the polymer molecules and the sol mixture results in composites with two different phases: silica gel network with polymer aggregates on the surface. These clusters of polymer molecules form additional scattering centers on the gel surface and thus cause opaque appearance. Eventually nonhomogenous composites are formed with poor optical properties.[25,26] This incompatibility can be overcome somewhat by eliminating the water from the reactant mixture like in the study of Jespersen et.al. who produced aeromosils having up to 75% PDMS(OH) by direct synthesis in $scCO_2$ without any water[27] or perhaps by using different solvents.

It is well-known that many silane compounds have appreciable solubility in $scCO_2$,[28−32] which can perhaps be exploited for development of new ways to synthesize composites of silica aerogels with silicone based polymers. In this study, a reactive supercritical deposition technique was employed to synthesize a composite of silica aerogel with PDMS. A functionalized form of PDMS, hydroxyl-terminated PDMS (PDMS(OH)), could be attached to the silica aerogel surface from the $scCO_2$ phase. The phase behavior of the PDMS(OH)-CO_2 binary mixture was investigated to determine the appropriate temperature, pressure and composition conditions for deposition from a single phase PDMS(OH)-CO_2 binary mixture. This data showed that PDMS(OH) and CO_2 forms miscible mixtures at a wide composition range at accessible pressures. The chemical attachment of the polymer onto the silica aerogel surface during supercritical deposition was verified by prolonged extraction with pure $scCO_2$, deposition using hydrophilic and superhydrophobic silica aerogel samples and ATR-FTIR analysis. In addition, the effects of deposition time and initial polymer concentration on the polymer uptake were investigated. The pore properties of the deposited samples were determined by N_2 sorption measurements. It was found that high polymer uptakes can be obtained depending on the deposition conditions. The novel reactive supercritical deposition technique allows for the production of monolithic, homogeneous and transparent silica-PDMS(OH) aerogel composites in a controlled manner which may pave the way for the utilization of silica aerogels and their composites in various applications such as core materials in transparent vacuum insulation panels.

■ MATERIALS AND METHODS

Materials. TEOS (98%) and hexamethyldisilizane (HMDS) (98%) were purchased from Alfa Aesar. Ethanol (99.9%) was purchased from Merck. Hydrochloric acid (HCl) (37%) was obtained from Riedel-de Haen and amonium hydroxide (NH_4OH) (2.0 M in ethanol) was obtained from Aldrich. PDMS(OH) (99.9%; kinematic viscosity (ν) = 65 mm^2/s; M_n = 2750 g/mol) was purchased from Sigma Aldrich. The chemicals were used as received. Carbon dioxide (99.998%) was purchased from Messer Aligaz.

Aparatus and Procedure for Demixing Pressure Measurements of PDMS(OH)-CO_2 Binary Mixture. The demixing pressure measurements were performed in a constant volume high pressure view cell. The view cell is a 2.8 cm diameter-cylindrical chamber, and it is equipped with two sapphire windows of 3.2 cm diameter at each side, poly(ether ether ketone) O-rings and a rupture disk. The volume of the high-pressure vessel is 57.64 ± 0.13 mL. Figure 1 displays the schematic of the experimental setup that was employed for the measurements. A syringe pump (Teledyne ISCO model: 260D) was used for the transfer of CO_2 into the high pressure vessel. The accuracy of the syringe pump pressure transducer was ±0.1 MPa and the accuracy for measuring the displaced volume was 0.5%. Another pressure transducer (Omega PX4100) and a thermocouple (Omega GTMQSS-062G-6) were employed to determine the temperature and pressure inside the vessel with a ±0.1 K and ±0.1 MPa accuracy. The temperature of the vessel was controlled by circulating water through the internal heating coils of the vessel using a circulating heater (Cole-Parmer model 12108-15). The temperature of the syringe pump was kept at 298 K by circulating water with a circulating heater (Cole-Parmer model 12108-15) through a jacket around the cylinder housing of the pump. The lines between the pump and the vessel were wrapped with insulating glass fiber to avoid temperature changes during the charging of CO_2. A magnetic stirrer was used to mix the contents of the vessel.

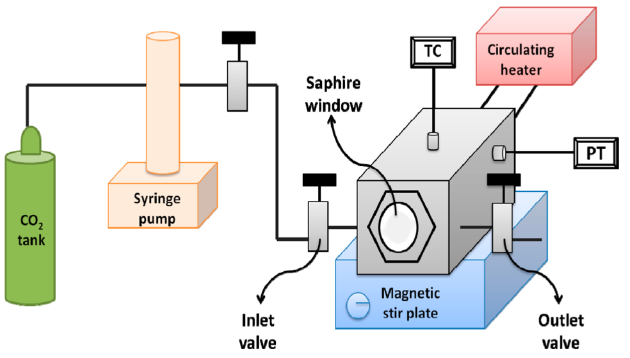

Figure 1. Experimental setup (TC, thermocouple; PT, pressure transducer).

Initially, a certain amount of polymer was weighed and placed inside the vessel. After it was sealed, the vessel was connected to the syringe pump. While keeping the inlet valve of the vessel closed, the syringe pump was started and the desired pressure was attained in the line between the syringe pump and the vessel. The inlet valve of the vessel was then opened and liquid CO_2 was charged into the vessel until the pressure inside the vessel reached the desired pressure value. Subsequently, the inlet valve was closed and the volume of CO_2 that was charged into the vessel was calculated from the change of the volume of the pump cylinder during the loading of CO_2. The mass of CO_2 that was transferred into the system was determined using the density of CO_2 at the pump conditions and the volume of CO_2 charged into the vessel. The density of CO_2 at the pump temperature and pressure was obtained from NIST database.[33] Consequently, the composition of the binary system was calculated from the masses of PDMS(OH) and CO_2 present inside the vessel. Following the addition of CO_2 at room temperature, the temperature of the vessel was brought to the experimental conditions using the circulating heater.

After a homogeneous, single-phase mixture of PDMS(OH) and CO_2 was attained inside the high pressure vessel, the outlet valve of the vessel was slightly opened and adjusted to have a slow rate of depressurization (~0.007 MPa/sec) at constant temperature. The compositions of the outlet stream and the mixture inside the vessel do not change during depressurization as long as the mixture is homogeneous and single-phase. During the depressurization of the vessel, the presence of the single phase system was continuously confirmed from the sapphire windows. At the phase separation point, white cloudy appearance of the binary mixture was visually detected and the pressure at that point was recorded as the cloud point pressure of the binary mixture at that composition and temperature. In addition to the cloud point, a bubble point was also observed at high PDMS(OH) weight fractions where a single bubble was observed at the top of the vessel chamber. The measurements were repeated for several compositions that were obtained by the addition of different amounts of PDMS(OH) and CO_2 to the vessel.

Synthesis of Silica Aerogels. Silica aerogels were synth esized by a two-step sol−gel procedure using TEOS as the silica precursor. Initially, TEOS was hydrolyzed with water in the presence of ethanol as the cosolvent and HCl as the acid catalyst. Subsequently, NH_4OH was added as the base catalyst to adjust the pH value of the sol mixture such that the condensation reactions were accelerated which eventually lead to the gelation of the solution. The molar ratios of TEOS/ethanol/H_2O/HCl/NH_4OH used in the synthesis were 1:4.52:3.94:0.002:0.01. After the addition of the base catalyst, the sol was poured into cylindrical syringe molds and let to gel. Following the gelation, the so-called alcogels were aged in 50:50 (v%) mixture of water and ethanol at 323.2 K for 24 h. Before the supercritical drying step, solvent exchange with pure ethanol was performed in order to replace the pore solvent. Lastly, ethanol was extracted from the pores with $scCO_2$ at 313.2 K and 9 MPa. Monolithic, crack-free and transparent silica aerogel samples were synthesized from the same batch. The samples had cylindrical shapes with 1.1 cm diameter and 1 cm height. The bulk density of the aerogels was 156 kg/m^3 and the BET surface area was measured as 1047 m^2/g.

Supercritical Deposition. The deposition experiments were performed with the same experimental setup that is displayed in Figure 1. The pressure and composition of the deposition experiments were determined according to the demixing pressure measurements carried out at 323.2 K in such a way that a single phase mixture was attained inside the vessel at the beginning and throughout the deposition process. All of the deposition experiments were performed at 323.2 K. Initially, a certain amount of polymer was placed into the vessel together with the silica aerogel sample and the vessel was brought to 323.2 K. A wire mesh was used to separate the aerogel sample from the polymer to avoid the contact of the sample with the liquid polymer which would destroy the aerogel structure. With continuous stirring, CO_2 was pumped into the vessel and the dissolution of the polymer in CO_2 occurred. When the desired pressure value was reached, a single phase binary mixture of PDMS(OH)-CO_2 was obtained in the vessel. The silica aerogel sample was exposed to this single phase mixture for varying durations. Typical volumes of the aerogel samples were around 1 mL. As the final step of the deposition, extraction with pure CO_2 was performed to remove the excess amount of polymer remaining in the vessel. The volume of pure CO_2 needed for complete extraction of the unreacted PDMS(OH) from the vessel was determined in separate experiments by passing varying amounts of CO_2. The phase behavior measurements showed that even if small amounts of PDMS(OH) existed in the mixture ($<w_{PDMS(OH)} = 0.01$), cloud points were observed during the depressurization of the vessel. Therefore, 5−6 vessel volume (~300 mL) of CO_2 was found to be sufficient to remove any unreacted polymer and no cloud points were observed during depressurization after the extraction. Furthermore, material balance calculations showed that the PDMS(OH) concentration in the fluid phase dropped to 1/200th of its initial value after passing 6 vessel volumes of CO_2 at a flow rate of 100 mL/h.

A hydrophobic silica aerogel reference sample was obtained by supercritical deposition of HMDS with CO_2.[34] The same experimental setup was utilized for HMDS deposition. The deposition was conducted with an initial HMDS amount of 2 mL at 333.2 K and 13.8 MPa for approximately 12 h. Following the deposition, supercritical extraction was carried out with 300 mL of pure CO_2 to remove the unreacted HMDS from the vessel. The superhydrophobicity of the aerogel sample was confirmed with a water droplet test.

The mass uptake values of all the deposited aerogel samples were determined gravimetrically. In addition, the attenuated total reflectance (ATR) Fourier transform infrared spectra (FTIR) were recorded on a Thermo Scientific Smart iTR to investigate the chemical composition of the samples. The pore properties of the samples were determined by N_2 adsorption−desorption measurements at 77 K (Micromeritics ASAP 2020). Prior to the analysis the samples were degassed at 353 K under vacuum for the removal of the impurities from the surface. The surface areas of the samples were determined with Brunauer−Emmett−Teller (BET) method whereas the pore volumes and pore size distributions were determined with Barrett−Joyner−Halenda (BJH) analysis from the N_2 adsorption−desorption isotherms. Total pore volumes were obtained by converting adsorbed N_2 volume at STP to liquid N_2 volume at 77 K. The contact angle measurements of the deposited samples were performed with Krüss contact angle measuring system (Krüss G10) by placing a droplet of triple distilled deionized water on the samples.

■ RESULTS AND DISCUSSION

Demixing Pressures of PDMS(OH)-CO_2 Binary Mixture. Initially, four subsequent demixing pressure measurements were performed using the PDMS(OH)-CO_2 binary mixture with the same composition ($w_{CO2} = 0.954$). The demixing pressure was determined as 27.6 ± 0.04 MPa which translates into a 0.2% standard deviation demonstrating the reproducibility of the data.

Further measurements were conducted to determine the demixing pressures of PDMS(OH)-CO_2 binary mixture for a wide composition range, up to a polymer content of 71 wt %. The demixing pressures measured at 323.2 K are displayed in Figure 2 for different CO_2 weight fractions. The demixing pressures were observed to decrease with the increasing polymer content at constant temperature. This trend is attributed to the much lower vapor pressure of PDMS(OH) compared to CO_2 which makes it the heavy component of the binary mixture. One important feature of this thermodynamic data is that it demonstrates that PDMS(OH) and CO_2 forms miscible mixtures over a wide composition range and indicates that it is possible to deposit PDMS(OH) from PDMS(OH)-CO_2 mixtures at accessible pressures.

Supercritical CO_2 Deposition of PDMS(OH) on to Silica Aerogels. As explained previously, the supercritical deposition method involves the dissolution of PDMS(OH) in $scCO_2$ and the exposure of silica aerogel to the single phase PDMS(OH)-CO_2 binary mixture. Deposition experiments with different initial PDMS(OH) concentrations were conducted at 323.2 K and 31 MPa for 24 h and the effect of the polymer

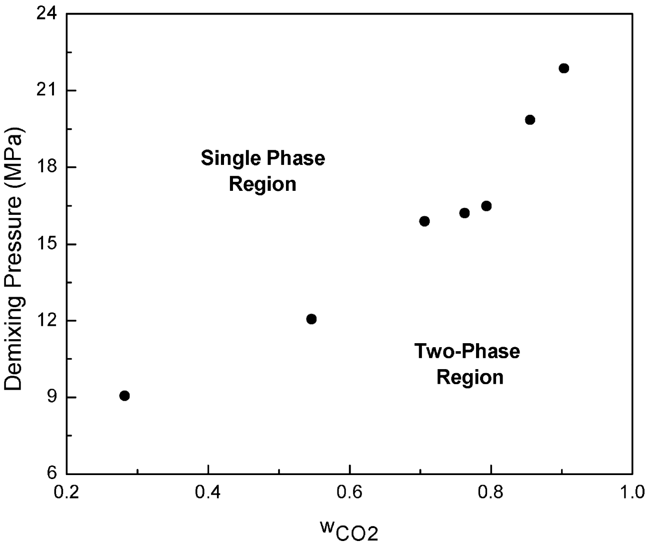

Figure 2. Demixing pressures of PDMS(OH)-CO_2 mixture at 323.2 K.

concentration on uptake amount was investigated. All of the deposited samples were obtained as monoliths and were crack-free. Figure 3 displays the mass uptakes of the aerogel samples for different polymer weight fractions and shows that there was almost a linear increase in mass uptake with increasing initial PDMS(OH) fraction. This increase in mass uptake can be attributed to the increasing concentration gradients between the bulk solution and the aerogel surface with increasing polymer weight fraction in solution which leads to enhanced rates of diffusion and/or reaction of the PDMS(OH) molecules.

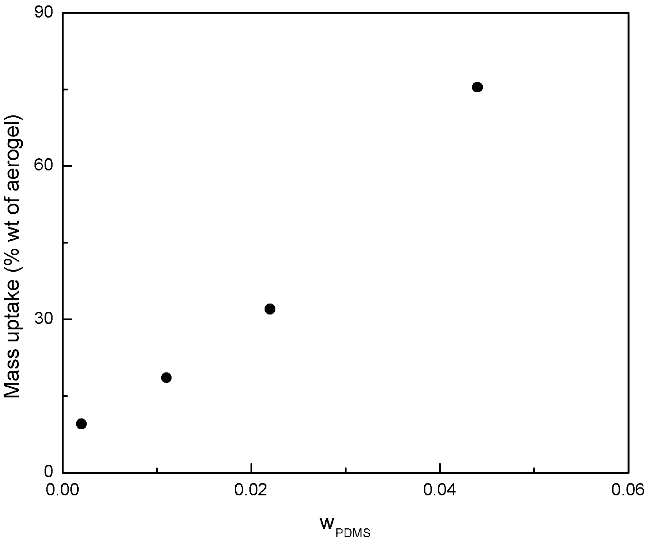

Figure 3. Mass uptake for different initial PDMS(OH) compositions in the vessel.

Polymer loading as high as 75.4 wt % was achieved which is quite high compared with the values reported in the literature for composites of PDMS(OH) with silica gel obtained by other methods.[24,27] To understand the reasons behind this substantial PDMS(OH) uptake of the silica aerogel, the mode of adsorption was investigated. In principal, there are two possible mechanisms through which PDMS(OH) can interact with the surface of the silica aerogel. The polymer molecules can either be covalently attached to the silica aerogel surface by a chemical bond which is formed by the reaction between the terminal −OH groups of PDMS(OH) and surface −OH groups of silica aerogel (chemisorption) or they can be adsorbed on the surface due to physical interactions without any chemical reaction (physisorption). One way to distinguish these two modes of adsorption is extraction with pure $scCO_2$. If adsorption is physisorption, then the deposited polymer can be extracted with pure CO_2 because of the reversible nature of physical adsorption and also because of the substantial solubility of PDMS(OH) in $scCO_2$. However, in the case of chemisorption, since the molecules are attached to the surface by chemical bonds, the polymer cannot be extracted with pure CO_2. Therefore, prolonged extraction of the aerogel sample with 75.4 wt % polymer uptake was performed with pure $scCO_2$ at 323 K in an Applied Separations Spe-ed SFE extraction unit in two stages for a total of 32 h. In the first stage supercritical extraction with CO_2 was performed at the deposition conditions for 12 h and the weight loss of the sample corresponded to 3.3% of the initial sample weight. The sample was then placed in the extractor and the extraction was continued for an additional 20 h. The weight loss of the sample was only 0.3 wt % of the sample weight. This weight loss is quite low compared to the initial mass uptake (75.4 wt %) which demonstrates that loaded polymer cannot be desorbed with further extraction. With the prolonged extraction of 32 h, a total of 6.6 mg of PDMS(OH) was extracted corresponding to 7.9% of the initially loaded polymer amount which can perhaps be attributed to the extraction of physisorbed polymer molecules. These results indicate that the major type of adsorption is chemisorption and the PDMS(OH) molecules react with the surface −OH groups and become attached to the silica aerogel surface. This reaction generates water which is either adsorbed on the silica aerogel surface or partitions into the fluid phase. In all the experiments, the amount of water generated was considerably smaller than the amount which could be dissolved in CO_2 based on the solubility data of water in $scCO_2$ at the experimental conditions (0.008 mol H_2O per mole of CO_2).[35]

ATR-FTIR analysis further supports the hypothesis of covalent bonding of the polymer with the aerogel surface. Figure 4 compares the ATR-FTIR spectra of the deposited aerogel samples with the native silica aerogel. There are two intense peaks that are specific to the chemical structure of silica and therefore occur in both spectra since both the backbone of the polymer and the solid silica network of the aerogel is made from silica. These peaks occur at 800 and 1080 cm^{-1} and are characteristic to Si−O−Si bending and stretching vibrations, respectively.[36] After deposition, the intensity of the peak at 800 cm^{-1} increases due to additional Si−O−Si bending vibrations of the polymer backbone. The broad band which appears at 3400 cm^{-1} originates from hydrogen bonded Si−OH with the adsorbed molecular water which is observed to weaken after the deposition of the polymer. More importantly, there are three peaks indicative of the presence of the polymer in the aerogel sample. The peak at 2963 cm^{-1} represents the C−H stretching vibrations originating from the methyl side groups of PDMS(OH). The peak at 1267 cm^{-1} is due to the Si−C stretching vibrations that originate from methyl side groups attached to the polymer backbone. The peak appearing at 850 cm^{-1} for the deposited sample was attributed to $\equiv$Si−O−$Si(CH_3)_2$−R bond that were formed due to the condensation reaction between the $\equiv$Si−OH groups of the aerogel and

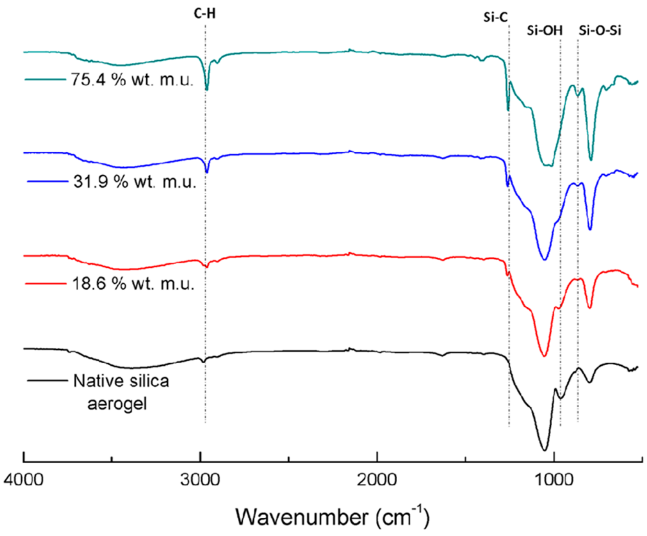

Figure 4. ATR-FTIR spectra showing the evolution of Si−C, C−H, and Si−O−Si peaks upon deposition.

OH−Si$(CH_3)_2$−R end groups of PDMS(OH).[36] The intensities of the C−H and Si−C stretching vibration peaks as well as the Si−O−Si peak that signifies the reaction between PDMS(OH) and surface −OH groups of the silica aerogel increased accordingly with the increasing polymer amount in the deposited samples. Furthermore, the peak at 960 cm^{-1} that was observed in native silica aerogel sample was attributed to stretching of Si−OH groups of the aerogel.[36,37] The disappearance of this peak upon deposition additionally indicates the reaction between PDMS(OH) and the surface Si−OH groups of the aerogel. The evolution of these specific peaks can be observed from the marked positions in Figure 4.

Further indication for the reaction of PDMS(OH) with surface −OH groups of the silica aerogel was obtained by a deposition experiment on a superhydrophobic and a hydrophilic silica aerogel simultaneously. Since the reaction of the polymer with the silica aerogel necessitates the presence of the surface −OH groups, removal of these groups, such as in the case of a superhydrophobic silica aerogel, would prevent this reaction and thus no polymer would be deposited on such superhydrophobic aerogels. Simultaneous deposition of PDMS(OH) on hydrophilic and superhydrophobic silica aerogel samples were performed at 323.2 K and 31 MPa for 24 h with $w_{PDMS(OH)}$ of 0.022% followed by supercritical extraction with pure CO_2. The mass uptake for the hydrophilic silica aerogel sample was 31.9 wt % whereas that of superhydrophobic silica aerogel sample was 3.9 wt %. The drastic difference between the mass uptake values of the two aerogel samples constitutes additional evidence that the PDMS(OH) molecules are chemically attached to the surface. The 3.9 wt % mass uptake observed for the superhydrophobic aerogel sample demonstrated that chemisorption also took place on the superhydrophobic surface due to the presence of some residual silanol groups, however the uptakes were small due to their small amount and poor accesibility. Figure 5 displays the images of the hydrophilic and superhydrophobic aerogel samples after the PDMS(OH) deposition. The higher amount of polymer in the hydrophilic aerogel sample was observed to decrease the transparency when compared to the superhydrophobic aerogel which contained a relatively small amount of polymer.

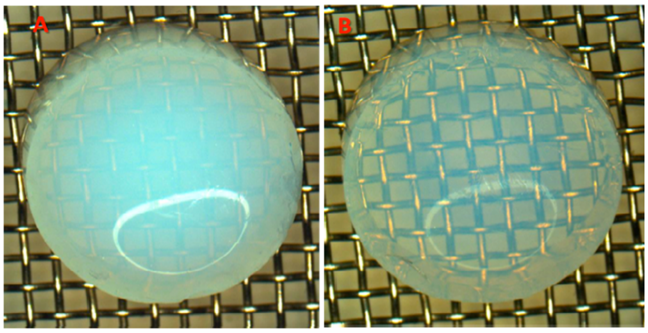

Figure 5. Images of (A) hydrophilic and (B) superhydrophobic aerogel samples after the deposition.

In addition, the effects of the deposition time on mass uptake were investigated by conducting deposition experiments for various durations. The experiments were performed at 31 MPa and 323.2 K with $w_{PDMS(OH)}$ of 0.022. Subsequently supercritical extraction with 300 mL of pure CO_2 was performed. Each deposition experiment was repeated three times. Figure 6 displays the mass uptakes for various deposition times with the standard deviations represented as the error bars for each data point. According to Figure 6, the mass uptakes increased with increasing deposition time. However, after 24 h the mass uptake seemed to be reaching an equilibrium value which indicated that with around 30 wt % of polymer uptake the aerogel surface became saturated with PDMS(OH) molecules and further elongation of the exposure time did not increase the uptake significantly. This behavior can originate from two possible situations; either almost all of the −OH groups on the aerogel surface reacted with the PDMS(OH) molecules or some of the surface −OH groups became inaccessible because of the polymer chains attached to the surface. For an uptake amount of 36 wt %, calculations indicated that approximately 8 PDMS(OH) molecules were present on 100 nm^2 of silica aerogel surface. Considering that there are approximately 500 −OH molecules per 100 nm^2 of native silica aerogel surface,[38−40] only a small fraction of surface −OH groups participated in reactions with PDMS(OH).

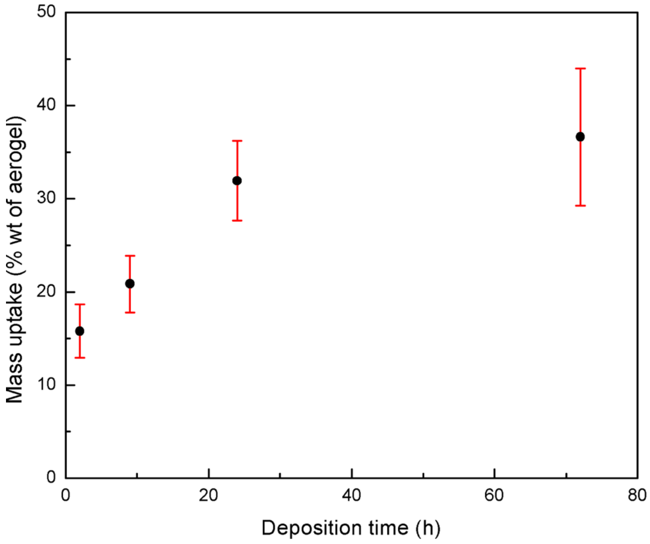

Figure 6. Mass uptake values for various deposition times.

The adsorption of polymers on inorganic surfaces is known to be quite a complicated process which is governed by different intermolecular interactions between the polymer and the surface.[41] The structure of polymer and surface, pH, temperature, the geometry of polymer, the topology of the surface, concentration and molecular weight of the polymer are some of the factors that govern the extent of adsorption and the structure of the adsorbed polymer phase.[42] When the polymer concentration on the surface is below the saturation point, the polymer chains adopt rather a flat conformation with enhanced number of interactions with the surface. With increased polymer concentration, the surface becomes saturated with the polymer chains which results in the entangled chains on the surface. The loop and tail portions of the entangled chains repel free polymer chains away from the surface because of the steric hindrance.[42]

There were some studies on the adsorption of PDMS on silica surfaces and the structure of the adsorbed PDMS layer. In some of these studies the PDMS chains were demonstrated to be partially adsorbed on the surface, that is, some segments of the polymer chain interact with the surface, while other segments are free and protrude from the surface. It was proposed that the segments that are not involved in the interactions with the surface can form loop like structures depending on the chain length of the polymer.[43−45] The adsorption of PDMS(OH) on silica surface was also investigated and it was proposed that the polymer chains can coat the silica surface forming a core−shell structure or can bind to each other forming bridges.[37] In any case, it is likely that a significant number of −OH groups on the silica surface are unavailable for new interactions either because they are involved in bonding with the polymer or are covered by the bound polymer chains.[43]

Regarding these considerations, it is likely that the chemisorbed PDMS(OH) molecules cover the unreacted surface −OH groups on aerogel surface and prevent the access of other PDMS(OH) molecules to these sites and therefore hinders their reactions. Another issue is the steric hindrance due to the crowding of the polymer molecules on the aerogel surface that may occur with increasing polymer loading. All these possible interactions can cause the saturation of the surface with polymer molecules as observed in the mass uptake results.

Figure 7 shows the images of aerogel samples that were deposited for 2, 9, and 72 h, with polymer contents of 15.8, 20.9, and 36.6 wt %, respectively. With increasing deposition time and thus the polymer content of the samples, the transparency decreased. During the depressurization, there occurs a transition from a good solvent medium ($scCO_2$) to a weak one (gaseous CO_2) which affects the structure and morphology of the adsorbed polymer layer. It is known that polymers adopt a brush-like structure in the presence of a good solvent and a mushroom-like, more closely packed structure in the presence of a weak solvent.[46−48] Therefore, it is possible for the reacted PDMS(OH) molecules to become entangled on the surface upon depressurization. One possible explanation for the decrease in transparency is that these entangled polymer molecules constitute additional scattering centers in the aerogel surface, which decreases the amount of light transmitted through the sample. Nonetheless, it is important to note that the transparency of the aerogels can be adjusted with the amount of polymer loaded and it is possible to obtain transparent aerogel composites at low polymer loadings. One of the most promising applications of silica aerogels is their utilization as core materials in transparent vacuum insulation panels. Therefore, being able to retain the transparency of the samples after the deposition is an essential feature of this technique that needs to be emphasized.

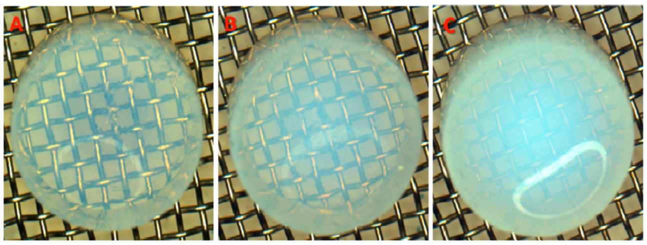

Figure 7. Images of aerogel samples with (A) 15.8 wt %, (B) 20.9 wt %, and (C) 36.6 wt % mass uptakes.

The homogeneity of the deposited samples, that is, whether the polymer molecules were homogenously distributed throughout the entire volume of the cylindrical samples, was also investigated. The visual observation of the cylindrical samples broken into two pieces indicated no nonhomogeneities in the appearance. Moreover, ATR-FTIR analyses were performed with the portions taken from the center and from the outer surface of the cylindrical sample. Figure 8 displays the spectra of the samples deposited for 72 h. It is evident that the spectra of the samples from the center and the outer surface overlap. The intensities of the specific peaks that are related to the polymer are identical indicating that the concentrations of the polymer molecules at the center and at the outer surface of the samples are similar. These results indicate that the polymer molecules penetrated to the center of the monoliths and were uniformly distributed.

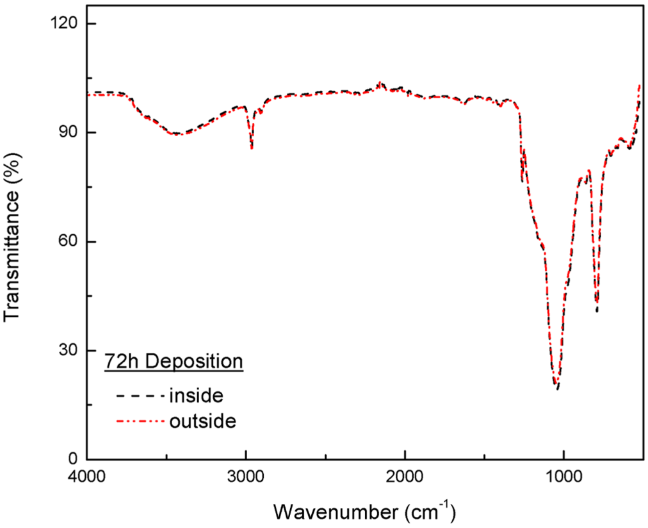

Figure 8. ATR-FTIR spectra of the samples from the center and outer surface of the monoliths deposited for 72 h.

The effects of mass uptake on the pore characteristics of the samples such as surface area, pore volume and pore size distribution were investigated by analyzing the N_2 adsorption−desorption isotherms. The analysis results were summarized in Table 1 together with the mass uptakes and densities. With increasing mass uptake the densities of the samples increased as

Table 1. Densities and Pore Characteristics of the Deposited Aerogels

mass uptake (wt% of aerogel)	density (kg/m^3)	BET surface area (m^2/g)	total pore volume (cm^3/g)
15.8	186	665	4.56
20.9	188	596	4.14
36.6	215	454	3.04
75.4	276	280	2.06

expected, whereas the surface areas and pore volumes decreased.

Furthermore, pore size distribution of the samples were obtained from the desorption branch of the isotherm by employing BJH method. Although both branches (adsorption and desorption) can be used for pore size calculations, from both a thermodynamic and historical point of view, the desorption branch is often favored for pore size assessment since the desorption process is more stable than the adsorption. However, both branches have been used in the studies on aerogels in the literature. It has been suggested that the adsorption of N_2 on the surface can cause contractions and can alter the structure of aerogels. Thus, the information extracted from desorption branch is more reliable. Furthermore, it has been known that if the hysteresis is of H1 type, the pore size distribution can be obtained both from adsorption and desorption branches. Moreover, the existence of H1 hysteresis (parallel adsorption and desorption branches of the isotherm) which is observed for the materials we developed in this study, indicates that the evaporation of the pore liquid occurs at thermodynamic equilibrium and there is no pore blocking, cavitation and percolation effects that contribute to hysteresis. For such cases, the desorption branch is generally utilized for the extraction of the pore size distribution. The pore size distributions of the samples were compared with the native silica aerogel in Figure 9 which shows that the average pore radius changed very slightly upon deposition. For comparison, the N_2 adsorption−desorption isotherms of the native silica aerogel and deposited aerogel with 36.6 wt % uptake were additionally given in Figure 9. It is clearly observed that the aerogel samples have Type IV isotherm with H1 type hysteresis loop with the desorption branch reflecting equilibrium capillary evaporation. The isotherms for the other the samples were similar but omitted for clarity.

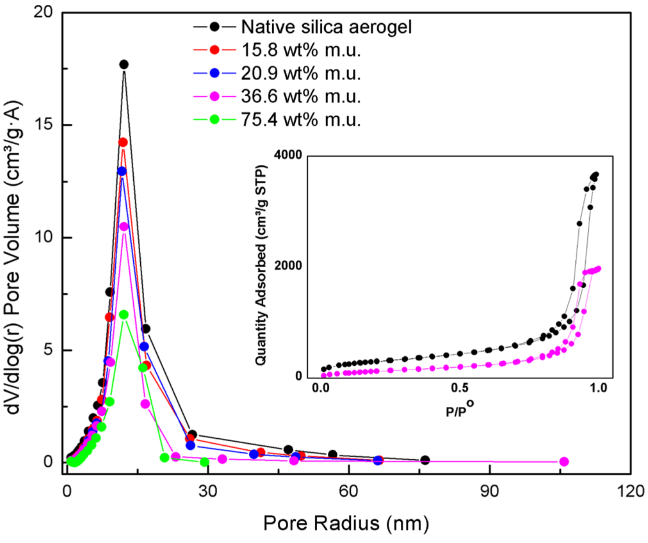

Figure 9. Pore size distribution and N_2 adsorption−desorption isotherms of the deposited samples (m.u. = mass uptake).

The volumes occupied by the polymer molecules in the pores were compared to the reductions in the pore volumes (the difference between the pore volumes of the native silica aerogel and the deposited samples as determined from N_2 adsorption−desorption isotherms by using BJH analysis). As shown in Figure 10, there is a very good match between those two volumes for all the samples. The slope of the best fit straight line through these points (the red dotted line) is 1.03 with an R-square value of 0.93. The closeness of the value of the slope to 1.0 shows that the volume of the PDMS(OH) molecules in the samples correspond to the reduction in the pore volumes, which occurred upon deposition.

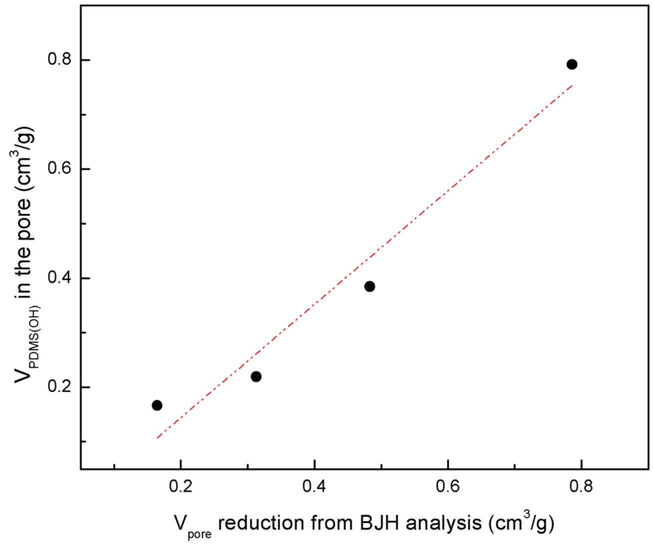

Figure 10. Correlation between volume of PDMS(OH) in the pores and pore volume reduction obtained from BJH analysis (red dotted line is the linear fit).

The analysis based on the pore size distribution revealed that there is a reduction in the pore volume for the entire pore size range and this volume reduction corresponds to the volume occupied by the deposited polymer molecules. These observations suggest some sort of conformal coating of the aerogel surface with the polymer molecules. In order to validate this coating hypothesis, the thickness of the coating layer was calculated for different pore sizes of each deposited sample by employing the BJH analysis results in the following manner. The thickness was calculated by dividing the polymer volume (volume corresponding to the difference between the pore volume of the deposited sample and the pore volume of the native silica aerogel) corresponding to a particular pore size range by the surface area of the native aerogel. Figure 11 displays the results obtained for each aerogel sample for the entire pore size range. The thickness of the polymer layer was found to be large (up to 14 nm) for the pores with radii larger than 26 nm. Moreover, the deviations in layer thicknesses of different polymer uptakes were calculated to be high for this pore size range. However, the contribution of the amount of polymer in these pores to the total polymer uptake were negligible for all the samples since the pores in this range are only 1% of the entire pores of the mesoporous silica aerogels. For pores smaller than 26 nm, the thickness of the polymer

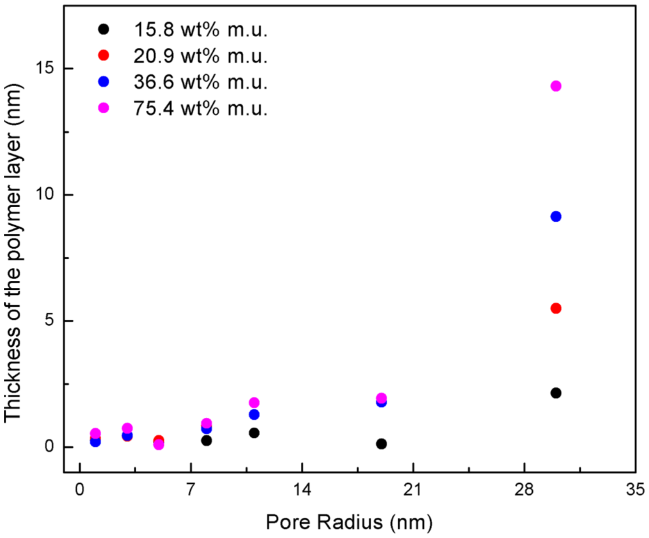

Figure 11. Thickness of the polymer layers for different pore sizes of the deposited samples.

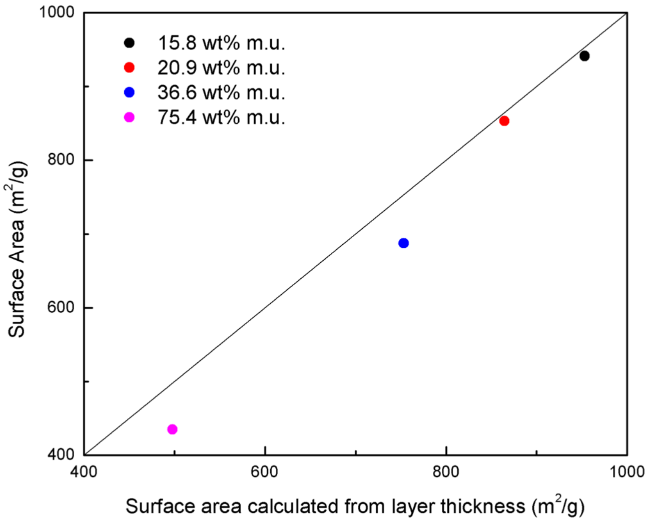

Figure 12. Surface areas of the samples obtained from BJH analysis and calculated from deposited layer thicknesses.

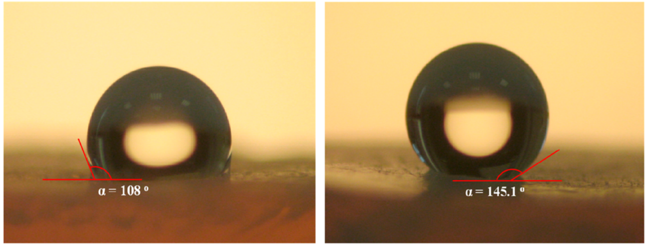

Figure 13. Water droplets on the deposited aerogels with 36.6 wt % (left) and 75.4 wt % (right) PDMS(OH).

layer fluctuated between 1 and 2 nm and seems to increase slightly with increasing mass uptake indicative of a conformal coating of 1−2 nm on the silica aerogel surface. The polymer layer thicknesses around 1−2 nm additionally explains the insignificant decreases of the average pore sizes displayed in Figure 9. The thickness of the polymer layer was also calculated from the adsorption branch of the N_2 sorption isotherms by following the same procedure. The calculated thicknesses were around 1 nm for the mesopore range and increased for larger pores. The calculated polymer layer thicknesses were further employed to determine the surface areas of the samples after the deposition. Spherical pore geometry was assumed in the calculations for simplicity and the surface areas of polymer coated samples were determined per gram of the composites. The pore radii used in the calculations were obtained by subtracting the coating thicknesses from the pore radii of the native silica aerogel. The results were compared with the surface areas obtained from BJH analysis, since BJH analysis results were utilized for the calculations of layer thicknesses. The good agreement between the calculated values and the analysis results displayed in Figure 12 verified the coating of the silica aerogel surface with polymer layer of the determined thicknesses. The deviations in Figure 12 most probably originate from the spherical pore geometry assumption which was a very crude assumption for the interconnected pore networks such as in the case of aerogels.

Silica aerogels are inherently highly hydrophilic due to the vast amount of −OH groups present on their surface. On the other hand, PDMS(OH) is a hydrophobic polymer with methyl side groups attached to the silica backbone. Coating the surface of the silica aerogels with a PDMS(OH) layer should cause an increase in the hydrophobicity of the surface. The contact angles of the two deposited samples with mass uptakes of 36.6 wt % and 75.4 wt % were measured along with the native silica aerogel and the results were shown in Figure 13. The native silica aerogel was completely wetted upon water contact. However, the contact angles for the samples with 36.6 wt % and 75.4 wt % polymer were determined to be 108° and 145.1°, respectively. The increasing contact angles with increasing amount of polymer in the samples was expected. Increased hydrophobicity is also important for use of these materials in transparent vacuum insulation panels.

■ CONCLUSION

Silica-PDMS(OH) composite aerogels were developed by employing a reactive supercritical deposition technique. The technique is composed of two stages; first stage is the dissolution of PDMS(OH) in CO_2 that results in a single phase binary mixture of PDMS(OH)-CO_2 in the vessel and the second stage is the exposure of the silica aerogel samples to the single phase binary mixture. During the course of the deposition, the polymer molecules were found to react with the surface −OH groups of the aerogel samples. It was shown that polymer uptakes as high as 75.4 wt % of aerogel could be attained depending on the composition of the initial binary mixture. The deposited samples retained their monolithic structure and the transparency of the aerogels could be preserved up to polymer loadings of around 20 wt %. In addition, the polymer uptake was determined to increase with increasing polymer weight fraction in the vessel and the deposition time. The deposited samples were characterized by ATR-FTIR and N_2-sorption analysis. Specific Si−C and C−H vibration peaks that originated from PDMS(OH) were identified in the ATR-FTIR spectra of the deposited samples and with the increasing polymer content in the samples the intensity of these peaks increased accordingly. Furthermore, it was demonstrated that the PDMS(OH) molecules could penetrate through the aerogel to the center of the cylindrical samples. The polymer molecules were determined to be homogenously distributed throughout the aerogel. According to the results obtained from N_2 adsorption−desorption isotherms, the specific surface area and the pore volume of the deposited samples decreased with increasing polymer content. It was understood from the BJH pore size distribution that the average pore size of the samples were affected very slightly by the polymer loading and the polymer molecules formed a layer on the aerogel surface. The thickness of the polymer layer was calculated for various pore sizes of each sample by employing BJH analysis results. It was found that the thickness of the polymer layer was higher for larger pores whereas there was a conformal coating with a thin polymer layer smaller than 1 nm for the smaller pores. The surface area after coating with the polymer was calculated by using the thicknesses of the polymer layer and was found to correspond to the surface area obtained from BJH analysis. In addition, the volume of the polymer loaded to the samples was correlated with the decrease in the pore volume obtained from the analysis of N_2 adsorption−desorption isotherms. According to these results, it was demonstrated that the volume of the PDMS-(OH) in the samples correspond to the reduction in the pore volume. All of these calculations indicate the conformal coating of the aerogel surface with a polymer layer. The deposited samples were also demonstrated to be hydrophobic and hydrophobicity increased with increasing polymer content. With the reactive supercritical deposition technique, various silane compounds can be employed in the surface modification of aerogels which may lead to the development of novel materials as well as novel processes to synthesize such materials.

■ AUTHOR INFORMATION

Corresponding Author

*E-mail: cerkey@ku.edu.tr.

Notes

The authors declare no competing financial interest.

■ ACKNOWLEDGMENTS

We acknowledge the Financial Support of the NANO-INSULATE (Development of Nanotechnology-based High-performance Opaque & Transparent Insulation Systems for Energy-efficient Buildings) being funded by the EU Program EeB.NMP.2010-1 under grant agreement no. (260086).

■ REFERENCES

(1) Fricke, J.; Emmerling, A. *Struct. Bonding (Berlin)* **1992**, *77*, 37.

(2) Dorcheh, A. S.; Abbasi, M. H. *J. Mater. Process. Technol.* **2008**, *199*, 10.

(3) Gurav, J. L.; Jung, I. K.; Park, H. H.; Kang, E. S.; Nadargi, D. Y. *J. Nanomater.* **2010**, *2010*, 1.

(4) Pierre, A. C.; Pajonk, G. M. *Chem. Rev.* **2002**, *102*, 4243.

(5) Baetens, R.; Jelle, B. P.; Gustavsen, A. *Energy Build.* **2011**, *43*, 761.

(6) Novak, B. M.; Auerbach, D.; Verrier, C. *Chem. Mater.* **1994**, *6*, 282.

(7) Wang, X.; Jana, S. C. *ACS Appl. Mater. Interfaces* **2013**, *5*, 6423.

(8) Martin, J.; Hosticka, B.; Lattimer, C.; Norris, P. M. *J. Non-Cryst. Solids* **2001**, *285*, 222.

(9) Nguyen, B. N.; Meador, M. A. B.; Medoro, A.; Arendt, V.; Randall, J.; McCorkle, L.; Shonkwiler, B. *ACS Appl. Mater. Interfaces* **2010**, *2*, 1430.

(10) Meador, M. A. B.; Fabrizio, E. F.; Ilhan, F.; Dass, A.; Zhang, G. H.; Vassilaras, P.; Johnston, J. C.; Leventis, N. *Chem. Mater.* **2005**, *17*, 1085.

(11) Meador, M. A. B.; Weber, A. S.; Hindi, A.; Naumenko, M.; McCorkle, L.; Quade, D.; Vivod, S. L.; Gould, G. L.; White, S.; Deshpande, K. *ACS Appl. Mater. Interfaces* **2009**, *1*, 894.

(12) Ilhan, U. F.; Fabrizio, E. F.; McCorkle, L.; Scheiman, D. A.; Dass, A.; Palczer, A.; Meador, M. B.; Johnston, J. C.; Leventis, N. *J. Mater. Chem.* **2006**, *16*, 3046.

(13) Katti, A.; Shimpi, N.; Roy, S.; Lu, H.; Fabrizio, E. F.; Dass, A.; Capadona, L. A.; Leventis, N. *Chem. Mater.* **2005**, *18*, 285.

(14) Zhang, G. H.; Dass, A.; Rawashdeh, A. M. M.; Thomas, J.; Counsil, J. A.; Sotiriou-Leventis, C.; Fabrizio, E. F.; Ilhan, F.; Vassilaras, P.; Scheiman, D. A.; McCorkle, L.; Palczer, A.; Johnston, J. C.; Meador, M. A.; Leventis, N. *J. Non-Cryst. Solids* **2004**, *350*, 152.

(15) Ge, D. T.; Yang, L. L.; Li, Y.; Zhao, J. P. *J. Non-Cryst. Solids* **2009**, *355*, 2610.

(16) Boday, D. J.; DeFriend, K. A.; Wilson, K. V.; Coder, D.; Loy, D. A. *Chem. Mater.* **2008**, *20*, 2845.

(17) Boday, D. J.; Stover, R. J.; Muriithi, B.; Keller, M. W.; Wertz, J. T.; Obrey, K. A. D.; Loy, D. A. *ACS Appl. Mater. Interfaces* **2009**, *1*, 1364.

(18) Boday, D. J.; Stover, R. J.; Muriithi, B.; Loy, D. A. *J. Mater. Sci.* **2011**, *46*, 6371.

(19) Nguyen, B. N.; Meador, M. A. B.; Tousley, M. E.; Shonkwiler, B.; McCorkle, L.; Scheiman, D. A.; Palczer, A. *ACS Appl. Mater. Interfaces* **2009**, *1*, 621.

(20) DeFriend, K. A.; Espinoza, B.; Patterson, B. *Fusion Sci. Technol.* **2007**, *51*, 693.

(21) Mulik, S.; Sotiriou-Leventis, C.; Churu, G.; Lu, H. B.; Leventis, N. *Chem. Mater.* **2008**, *20*, 5035.

(22) Fidalgo, A.; Farinha, J. P. S.; Martinho, J. M. G.; Rosa, M. E.; Ilharco, L. M. *Chem. Mater.* **2007**, *19*, 2603.

(23) Liu, Y.; Chen, H.; Zhang, L.; Yao, X. *J. Sol−Gel Sci. Technol.* **2002**, *25*, 95.

(24) Kramer, S. J.; RubioAlonso, F.; MacKenzie, J. D. In *Better Ceramics through Chemistry VII: Organic/Inorganic Hybrid Materials*; Coltrain, B. K., Sanchez, C., Schaefer, D. W., Wilkes, G. L., Eds.; Materials Research Society: Pittsburgh, PA, 1996; Vol. 435, p 295.

(25) Dong, W.; Faltens, T.; Pantell, M.; Simon, D.; Thompson, T.; Dong, W. *MRS Online Proc. Libr.* **2009**, 1188.

(26) Characterization and Properties of Sol−Gel Materials and Products. *Handbook of Sol−Gel Science and Technology: Processing, Characterization and Applications*; Almeida, R. M., Ed.; Kluwer Academic Publishers: New York, 2005; Vol. *II*.

(27) Jespersen, H. T.; Standeker, S.; Novak, Z.; Schaumburg, K.; Madsen, J.; Knez, Z. *J. Supercrit. Fluids* **2008**, *46*, 178.

(28) Miller, M. B.; Luebke, D. R.; Enick, R. M. *Energy Fuels* **2010**, *24*, 6214.

(29) Garcia-Gonzalez, C. A.; Fraile, J.; Lopez-Periago, A.; Saurina, J.; Domingo, C. *Ind. Eng. Chem. Res.* **2009**, *48*, 9952.

(30) Cao, C. T.; Fadeev, A. Y.; McCarthy, T. J. *Langmuir* **2001**, *17*, 757.

(31) Miller, M. B.; Chen, D. L.; Xie, H. B.; Luebke, D. R.; Johnson, J. K.; Enick, R. M. *Fluid Phase Equilib.* **2009**, *287*, 26.

(32) Dzielawa, J. A.; Rubas, A. V.; Lubbers, C.; Stepinski, D. C.; Scurto, A. M.; Barrans, R. E.; Dietz, M. L.; Herlinger, A. W.; Brennecke, J. F. *Sep. Sci. Technol.* **2008**, *43*, 2520.

(33) Linstrom, P. J.; Mallard, W. G. Unpublished work, 2011.

(34) Kartal, A. M.; Erkey, C. *J. Supercrit. Fluids* **2010**, *53*, 115.

(35) Wiebe, R. *Chem. Rev.* **1941**, *29*, 475.

(36) Mosquera, M. J.; de los Santos, D. M.; Rivas, T. *Langmuir* **2010**, *26*, 6737.

(37) Zhang, X. X.; Xia, B. B.; Ye, H. P.; Zhang, Y. L.; Xiao, B.; Yan, L. H.; Lv, H. B.; Jiang, B. *J. Mater. Chem.* **2012**, *22*, 13132.

(38) Kulkarni, M. M.; Bandyopadhyaya, R.; Bhattacharya, B.; Sharma, A. *Acta Mater.* **2006**, *54*, 5231.

(39) Brinker, C. J.; Scherer, G. W. *Sol−Gel Science*; Academic Press: San Diego, CA, 1990.

(40) *Aerogel Handbook*; Aegerter, M. A., Leventis, N., Koebel, M., Eds.; Springer Science+Business Media: New York, 2011.

(41) Al Akoum, R.; Vaulot, C.; Schwartz, D.; Hirn, M. P.; Haidar, B. *J. Polym. Sci., Part B: Polym. Phys.* **2010**, *48*, 2371.

(42) Parida, S. K.; Dash, S.; Patel, S.; Mishra, B. K. *Adv. Colloid Interface Sci.* **2006**, *121*, 77.

(43) Levresse, P.; Feke, D. L.; Manas-Zloczower, I. *Polymer* **1998**, *39*, 3919.
(44) Litvinov, V. M.; Barthel, H.; Weis, J. *Macromolecules* **2002**, *35*, 4356.
(45) Panja, D.; Barkema, G. T.; Kolomeisky, A. B. *J. Phys.: Condens. Matter* **2009**, *21*, 242101.
(46) Hsu, H. P.; Paul, W.; Binder, K. *J. Phys. Chem. B* **2011**, *115*, 14116.
(47) Auroy, P.; Auvray, L.; Leger, L. *Macromolecules* **1991**, *24*, 5158.
(48) Karim, A.; Tsukruk, V. V.; Douglas, J. F.; Satija, S. K.; Fetters, L. J.; Reneker, D. H.; Foster, M. D. *J. Phys. II* **1995**, *5*, 1441.